

# Single Particle and Collective Structure for Nuclei near $^{132}\text{Sn}$

Jing-ye Zhang<sup>(1)</sup>, Yang Sun<sup>(1)</sup>, Mike Guidry<sup>(1,2)</sup>, L.L. Riedinger<sup>(1)</sup>, and G.A. Lalazissis<sup>(3)</sup>

<sup>(1)</sup>*Department of Physics and Astronomy, University of Tennessee, Knoxville, Tennessee 37996*

<sup>(2)</sup>*Physics Division, Oak Ridge National Laboratory, Oak Ridge, Tennessee 37831*

<sup>(3)</sup>*Physik-Department, Technische Universität München, D-85747 Garching, Germany*

(October 25, 2018)

## Abstract

A new Nilsson single-particle structure is proposed for neutron-rich nuclei near  $^{132}\text{Sn}$ . In general, a large reduction in spin-orbit interaction is required and the neutron  $N = 82$  gap persists in the new set of parameters. The ground state deformations for several isotopic chains are studied with this set and compared with the results of the standard set and with measured ones. Collective bands in two even-even, neutron-rich nuclei are calculated using the Projected Shell Model with the new set of parameters and improved agreement with existing data is found.

The study of nuclei far from  $\beta$ -stability is an important topic in nuclear physics [1], both because of their intrinsic importance to nuclear structure and for their importance in astrophysics. One substantial step along this line is to investigate the neutron rich nuclei where data are available, such as those around  $^{132}\text{Sn}$ . These nuclei are of unique interest because  $^{132}\text{Sn}$  is expected to have doubly closed shells and the levels in nearby nuclei are expected to be largely of single-particle nature. We note in this regard that the  $3^-$  state in  $^{132}\text{Sn}$  lies at 4.3512 MeV, much higher than in  $^{208}\text{Pb}$  (2.6146 MeV) [2]. Thus,  $^{132}\text{Sn}$  may be expected to be an even better closed shell nucleus than  $^{208}\text{Pb}$ . Therefore, as an approximation, the single particle and hole states observed experimentally in the nearest odd-A nuclei are assumed to be pure in structure, and can be directly used as references to

construct the theoretical single particle scheme for this region [3].

For the  $^{132}\text{Sn}$  region, some experimental data are beginning to fill the gaps between the known single-particle spectrum in the stability valley and the unknown spectrum at the drip line. For example, the single-particle structure above and below the neutron number  $N = 82$  gap can be found from decay data for  $^{133}\text{Sn}$  [4] and  $^{131}\text{Sn}$  [5]. However, near the proton  $Z = 50$  gap, less is known; only a few particle states from  $^{133}\text{Sb}$  [7,3] and one hole state from  $^{131}\text{In}$  [8,5] have been reported. This paper proposes to construct a new single-particle spectrum utilizing available experimental data, and to investigate the impact of this spectrum on ground state properties and collective excitations in the region near  $^{132}\text{Sn}$ .

The Nilsson model with the “standard” set of parameters [9,10] has been quite successful in describing the single-particle structure for stable nuclei. Two parameters,  $\kappa$  and  $\mu$ , appear in the Nilsson potential

$$V = -\kappa\hbar\omega_0^\pm [2l_t \cdot s + \mu(l_t^2 - \langle l_t^2 \rangle_N)] \quad (1)$$

$$\hbar\omega_0^\pm = \hbar\omega_0 [1 \pm (N - Z)/3A] \quad (2)$$

where “+” stands for neutrons and “-” for protons,  $\hbar\omega_0$  is the harmonic-oscillator parameter,  $s$  is the intrinsic nucleon spin, and  $l_t$  is the orbital angular momentum in the stretched coordinate basis [9]. However, the experimental information for nuclei near  $^{132}\text{Sn}$  indicates that the standard parameter set cannot be correct for very neutron-rich nuclei. Thus, an adjustment of these parameters is necessary if one hopes to describe this region using a Nilsson single-particle spectrum.

Let us first consider the neutron single-particle structure. To reproduce the observed single-neutron particle levels above the  $N = 82$  gap, one must reduce the strength of the spin-orbit interaction for  $N = 5$  with  $l = 1$  and  $l = 3$  substantially from the standard value in the stability valley because of the observed smaller separation between  $f_{7/2}$  and  $f_{5/2}$  levels, and between  $p_{3/2}$  and  $p_{1/2}$  orbitals. On the other hand, the pair of  $h$ -orbitals require a larger value of  $\kappa$  to position them properly above the gap ( $h_{9/2}$ ) and below it ( $h_{11/2}$ ). For other orbitals below the  $N = 82$  gap, one also requires a reduction in  $\kappa$ .

It is crucial to notice that, from Eq. (1), if  $\mu \leq 0.50$  the energy order of neutron orbitals is  $d_{5/2}, g_{7/2}, s_{1/2}, d_{3/2}$ , while for  $\mu > 0.50$ , the energy order is  $g_{7/2}, d_{5/2}, d_{3/2}, s_{1/2}$ . Therefore, the  $\mu$  parameter for the  $s, d$  shells and for the  $g$  shell *cannot* be the same if the experimental energy order of  $g_{7/2}, d_{5/2}, s_{1/2}, d_{3/2}$  [5] is to be reproduced; in particular, the  $g_{7/2}$  orbital is required by the data to be about 800 keV below the  $d_{5/2}$  orbital. The necessity of introducing the  $l$ -dependent Nilsson parameters has been pointed out in Ref. [6] too. For proton single-particle levels near  $Z = 50$  the experimental information is less extensive and a reduction of  $\kappa(N = 4, 5)$  plus an adjustment of  $\mu(N = 3, 4, 5)$  are necessary to reproduce the limited set of known particle and hole spectra. However, since at present we don't have further experimental information about the size of  $Z = 50$  gap, we still keep the standard kappa value for the pair of  $g$ -orbitals. In Table I, we summarize the adjusted proton and neutron  $\kappa$  and  $\mu$  parameters for the  $N = 3, 4$ , and  $5$  shells that best reproduce the available data in this region. According to the most probable spin and parity assignment for the parent state in  $^{134}\text{In}$ , the neutron separation energy in  $^{133}\text{Sn}$ , and the semiempirical Woods-Saxon potential adjusted from the data near  $^{208}\text{Pb}$  [4], the  $\nu i_{13/2}$  orbital should lie above 3 MeV in excitation. In our case, the  $N = 6$  shell has not been modified and lies at 3.4 MeV relative to the  $\nu f_{7/2}$  orbital, in a position consistent with all available information. Table II shows the corresponding single-particle level scheme from the experimental data, that from the new Nilsson parameters, and that derived from the standard set of parameters [9,10], for nuclei around  $^{132}\text{Sn}$ . Obviously, the new set of parameters nicely reproduces the data while the standard set does not.

Relativistic Mean Field (RMF) theory [11] with nonlinear self-interactions between mesons has been used in many studies of low-energy phenomena in nuclear structure. A careful investigation of isospin dependence for the spin-orbit interaction in neutron-rich nickel and tin isotopic chains indicates that the spin-orbit potential is considerably reduced, resulting in smaller energy splittings between spin-orbit partners [12]. The spin-orbit interaction, which is central to the preceding discussions, arises naturally in RMF theory as a result of the Dirac structure of the nucleons. Thus, it is relevant to consider the relation of

the new single-particle Nilsson spectrum to that of the RMF.

The single-particle levels from RMF calculations with three typical interactions [11,12] (NL1, NL3, NLSH) are listed in Table II as well. Without any special parameter adjustment for this particular region, the RMF single-particle levels are found to be reasonably close to the data. Furthermore, the results from both our new  $\kappa, \mu$  Nilsson parameter set and the RMF indicate a smaller separation between spin-orbit partners that originates from a reduction of the spin-orbit interaction strength (except for our special adjustment of the neutron  $\kappa$  for  $N = 5$  to separate the  $h_{11/2}$  and  $h_{9/2}$  orbitals for the reasons mentioned above). The  $N = 82$  gap survives in the new set of Nilsson parameter, as is also true in the RMF [13] and in the FRDM [14] for these neutron-rich nuclei. Fig. 1 shows the experimental neutron level scheme around the 82 gap as well as calculated Nilsson levels with the standard set and proposed set of parameters and the onset from RMF calculation with NL3 parameters. It is obvious that the new set of parameters reproduces well the observed particle and hole state levels.

Next, we consider the impact of the new Nilsson parameters on other physical quantities. Fig. 2 shows deformations extracted from Potential Energy Surface calculations for cadmium, tellurium and xenon isotopes by the usual Nilsson-Strutinsky-BCS approach [9], employing both the new and the standard  $\kappa$  and  $\mu$  parameter sets. For reference, deformations extracted from experimental quadrupole moment values [15] by an empirical formula [16] are included too. Unfortunately, the experimental deformations so far observed are mostly for stable nuclei and hence can't be used to check the new set of parameters. However, the overall difference between calculated deformations from the two sets of parameters is not large, implying that global ground-state properties of even-even nuclei such as the deformation are not very sensitive to the details of the single-particle structure. Therefore, the validity of the new parameter set should be further checked by comparing with other quantities that provide a more stringent test of the single-particle structure.

The new Nilsson parameters should represent a better basis from which more sophisticated wave functions can be constructed. Therefore, we may test the new Nilsson parameters

by employing them in calculations that have a direct connection with measured collective spectra. For this purpose, we shall employ the Projected Shell Model (PSM) to calculate the yrast bands of two even–even nuclei,  $^{136}\text{Te}$  and  $^{142}\text{Xe}$ , for which limited data are available.

The PSM [17] is a spherical shell model truncated in a deformed Nilsson–BCS basis. This truncation is highly efficient if the single-particle basis is realistic because the quasiparticle basis already contains most of the correlations [17]. Therefore, the quality of the Nilsson single-particle states is crucial for the PSM results. Once a good single-particle basis is provided to the PSM, energy levels and many-body wave functions can be obtained through shell model diagonalization. It has indeed been shown that the PSM can nicely describe the collective bands in normally deformed [17], superdeformed [18], and transitional nuclei [19]. This further permits the matrix elements for processes such as electromagnetic transitions and direct capture to be calculated as well.

In PSM calculations of the low-spin states relevant here, the projected multi-quasiparticle states consist of 0- and 2-qp ( $2\nu$  and  $2\pi$ ) states for even–even nuclei, typically with a dimension of 50. For the single-particle space we use three major shells:  $N = 4, 5,$  and  $6$  for neutrons and  $N = 3, 4,$  and  $5$  for protons. The deformations in the Nilsson single-particle basis were  $\varepsilon_2 = 0.060$  and  $\varepsilon_4 = -0.004$  for  $^{136}\text{Te}$ , and  $\varepsilon_2 = 0.150$  and  $\varepsilon_4 = -0.012$  for  $^{142}\text{Xe}$ . These values are consistent with those presented in Fig. 2. All the states within one nucleus were obtained from the diagonalization in this (projected) shell model basis with the same basis deformation.

Fig. 3 shows results from the PSM calculation. It is obvious that the calculations employing the new set of Nilsson parameters nicely reproduce the data, while those with the standard set of Nilsson parameters determined in the stability valley are in much poorer agreement. More important than the quantitative differences is that the qualitative nature of the collective excitations is very different for the two parameter sets. For example, in  $^{142}\text{Xe}$ , the new set gives (correctly) a more rotational structure, while the older set suggests a more vibrational structure, even though the calculated deformations are very similar. Here it is the change in single particle states that gives rise to the different nature of the yrast

sequence.

Around the mass-140 region, especially near  $Z = 56$ , octupole degrees of freedom have been found to be important in earlier calculations [20,21,14]. In the present PSM calculation, the octupole degree of freedom has not been included. Therefore, the number of nuclei that can be used to examine the proposed Nilsson parameter set has been restricted to nuclei that are expected to have little octupole coupling. We note that the separation between the two key orbitals that is responsible for the main octupole correlation in the mass region discussed,  $\nu i_{13/2}$  and  $\nu f_{7/2}$ , is about 1 MeV larger from the new set of parameters than that from the standard one (see table II), which should result in a weaker octupole correlation. Therefore we do not expect the inclusion of octupole forces to alter our discussion of the examples shown here. In the future, one should investigate quantitatively the influence of octupole deformation on the yrast band spectra for this neutron-rich mass region based on the new set of Nilsson parameters with larger separation of the  $\nu i_{13/2}$  and  $\nu f_{7/2}$  orbitals.

Because of the limited present information on empirical single-particle spectra in this region, this new set of parameters should be employed with confidence only for neutron-rich nuclei with  $Z = 46 - 56$  and  $N = 68 - 96$ . Furthermore, the present parameterization is on firmer ground for nuclei with proton number beyond 50, since there is only one hole state known experimentally below the  $Z = 50$  gap. Nevertheless, the evidence cited above suggests that a parameterization at least similar to the one presented here will be required to describe the physics of this entire region of neutron-rich nuclei.

In summary, a new set of Nilsson parameters is proposed for neutron-rich nuclei around  $^{132}\text{Sn}$ . These parameters differ substantially from those commonly employed for stable nuclei, and nicely reproduce the existing data. Reduced separation between spin-orbit partners and persistence of the neutron  $N = 82$  gap are found in the new Nilsson diagram. We find many similarities between the new single-particle scheme and results from Relativistic Mean Field Theory. Available data for yrast bands in even-even nuclei around  $^{132}\text{Sn}$  are well reproduced by PSM calculations with the new set of Nilsson states as a basis, but the spectra are not even qualitatively in agreement with data when the standard set is used. However, the nuclei

that can be used to examine the proposed parameter set is quite limited at present, and it is obvious that more experimental data are needed to further fix the Nilsson parameters for these neutron rich nuclei. Improvements in the theoretical model, such as the inclusion of the octupole degree of freedom is required as well.

#### **ACKNOWLEDGMENTS**

We thank Drs. C. Bingham, J. Dobaczewski and C. L. Wu for valuable discussions. Research at the University of Tennessee is supported by the U. S. Department of Energy through Contract No. DE-FG05-96ER40983. Oak Ridge National Laboratory, is managed by Lockheed Martin Energy Research Corp. for the U. S. Department of Energy under Contract No. DE-AC05-96OR22464.

## REFERENCES

- [1] P.G. Hansen, *Ann. Rev. Nucl. Part. Sci.* **29**, 69 (1979).
- [2] R.B. Firestone *et al.*, *Table of Isotopes*, 8th edition (John Wiley & Sons, Inc., 1996).
- [3] M. Sanchez-Vega *et al.*, *Phys. Rev. Lett.* **80**, 5504 (1998).
- [4] P. Hoff *et al.*, *Phys. Rev. Lett.* **77**, 1020 (1996).
- [5] B. Fogelberg and J. Blomqvist, *Nucl. Phys.* **A429**, 205 (1984).
- [6] T. Seo, *Z. Phys.* **A324**, 43 (1986).
- [7] J. Blomqvist, A. Kerek and B. Fogelburg, *Z. Phys.* **A314**, 199 (1983).
- [8] E. Lund *et al.*, *Z. Phys.* **A294**, 233 (1980).
- [9] S.G. Nilsson *et al.*, *Nucl. Phys.* **A131**, 1 (1969).
- [10] T. Bengtsson and I. Ragnarsson, *Nucl. Phys.* **A436**, 14 (1985).
- [11] P. Ring, *Prog. Part. Nucl. Phys.* **37**, 193 (1996).
- [12] G.A. Lalazissis *et al.*, *Phys. Lett.* **B418**, 7 (1998); *Phys. Rev.* **C57**, 2294 (1998).
- [13] M.M. Sharma, G.A. Lalazissis, W. Hillebrandt, and P. Ring, *Phys. Rev. Lett.* **72** (1994) 1431
- [14] P. Möller *et al.*, *Atom. Data and Nucl. Data Tables* **59**, 185(1995).
- [15] S. Raman *et al.*, *Atomic Data and Nuclear Data Tables* **36**, 1 (1987).
- [16] K. Lobner *et al.* *Nucl. Data Tables* **A7**, 495 (1970). **59**, 185 (1995).
- [17] K. Hara and Y. Sun, *Int. J. Mod. Phys.* **E4**, 637 (1995).
- [18] Y. Sun, J.-y. Zhang and M. Guidry, *Phys. Rev. Lett.* **78**, 2321 (1997).
- [19] Jing-ye Zhang *et al.*, *Phys. Rev* **C52**, R2330 (1995).
- [20] J.L. Egido and L.M. Robledo, *Nucl. Phys.* **A518**, 465 (1990).
- [21] B.A. Butler and W. Nazarewicz, *Nucl. Phys.* **A533**, 249 (1991).



## FIGURES

FIG. 1. Single neutron particle (a) and hole(b) states. Experimental (left-most) and calculated results from Nilsson model with new parameter set, from standard set, and from RMF with NL3 parameterization.

FIG. 2. Ground state deformations: experimental values [15] (dots), absolute values from calculations with new set of parameters (open triangles), and with standard parameter set (open circles) for Cd, Te and Xe isotopes.

FIG. 3. Yrast bands in  $^{136}\text{Te}$  and  $^{142}\text{Xe}$  from experimental data (dots) [2] and PSM calculations with the new set of Nilsson parameters (open triangles), and with the standard Nilsson parameters (open circles).

TABLES

TABLE I. Nilsson Parameters  $\kappa$  and  $\mu$  around  $^{132}\text{Sn}$

| N | $l$ | $\kappa_p$ | new $\kappa_p$ | $\mu_p$ | new $\mu_p$ | $\kappa_n$ | new $\kappa_n$ | $\mu_n$ | new $\mu_n$ |
|---|-----|------------|----------------|---------|-------------|------------|----------------|---------|-------------|
| 3 | 1,3 | 0.090      |                | 0.300   | 0.340       | 0.090      |                | 0.250   |             |
| 4 | 0,2 | 0.065      | 0.039          | 0.570   | 0.760       | 0.070      | 0.039          | 0.390   | 0.330       |
|   | 4   |            | 0.065          |         |             |            |                |         | 1.089       |
| 5 | 1,3 | 0.060      | 0.052          | 0.650   | 0.645       | 0.062      | 0.035          | 0.430   | 0.090       |
|   | 5   |            |                |         |             |            | 0.082          |         | 0.490       |

TABLE II. Level Scheme of  $^{131}\text{Sn}$  (neutron hole),  $^{133}\text{Sn}$  (neutron particle),  $^{131}\text{In}$  (proton hole) and  $^{133}\text{Sb}$  (proton particle)

|                  | orbital    | exp.   | new $\kappa, \mu$ | old $\kappa, \mu$ | NL1    | NL3    | NLSH   |
|------------------|------------|--------|-------------------|-------------------|--------|--------|--------|
| $\nu$ -<br>hole  | $d_{3/2}$  | 0.000  | 0.000             | 0.000             | 0.000  | 0.000  | 0.000  |
|                  | $h_{11/2}$ | -0.242 | -0.265            | -0.044            | +2.019 | +1.249 | +0.446 |
|                  | $s_{1/2}$  | -0.332 | -0.346            | -0.403            | +0.308 | +0.423 | +0.461 |
|                  | $d_{5/2}$  | -1.655 | -1.695            | -3.047            | -1.623 | -1.657 | -1.759 |
|                  | $g_{7/2}$  | -2.434 | -2.435            | -2.108            | -2.309 | -3.403 | -4.224 |
| $\nu$ -<br>part. | $f_{7/2}$  | 0.000  | 0.000             | 0.000             | 0.000  | 0.000  | 0.000  |
|                  | $p_{3/2}$  | 0.854  | 0.883             | 3.399             | 0.868  | 0.860  | 0.702  |
|                  | $h_{9/2}$  | 1.561  | 1.481             | 0.681             | 1.956  | 0.956  | 0.369  |
|                  | $p_{1/2}$  | 1.656  | 1.797             | 5.018             | 1.203  | 1.202  | 1.033  |
|                  | $f_{5/2}$  | 2.005  | 2.122             | 3.777             | 1.468  | 1.434  | 1.312  |
|                  | $i_{13/2}$ |        | 3.408             | 2.476             | 4.729  | 3.951  | 3.266  |
| $\pi$ -<br>hole  | $g_{9/2}$  | 0.000  | 0.000             | 0.000             | 0.000  | 0.000  | 0.000  |
|                  | $p_{1/2}$  | -0.363 | -0.358            | -1.102            | -1.546 | -1.010 | -0.426 |
| $\pi$ -<br>part. | $g_{7/2}$  | 0.000  | 0.000             | 0.000             | 0.000  | 0.000  | 0.000  |
|                  | $d_{5/2}$  | 0.962  | 0.965             | 0.472             | 1.851  | 2.814  | 3.563  |
|                  | $d_{3/2}$  | 2.440  | 2.408             | 2.880             | 3.534  | 4.503  | 6.257  |
|                  | $h_{11/2}$ | 2.793  | 2.772             | 1.536             | 4.331  | 4.611  | 4.629  |

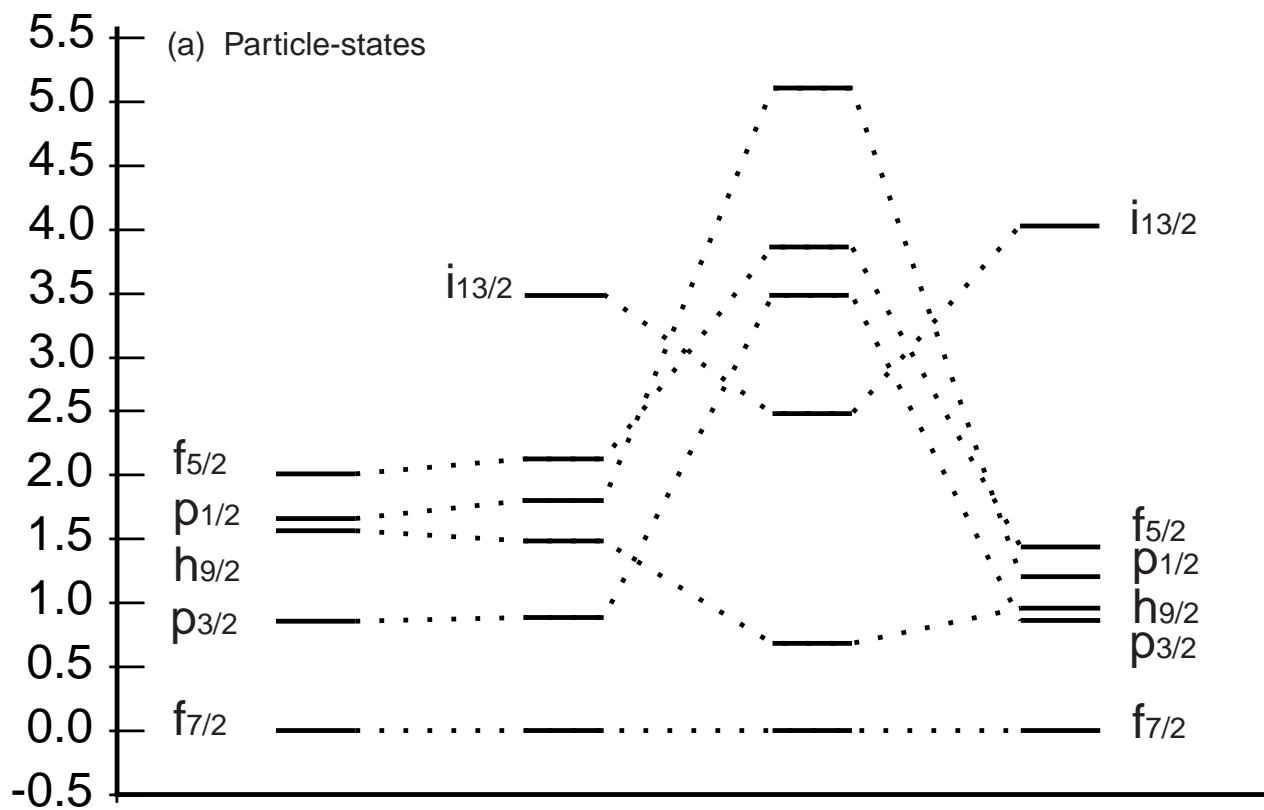


Fig. 1a, Zhang, Sun, Guidry, Riedinger, Lalazissis

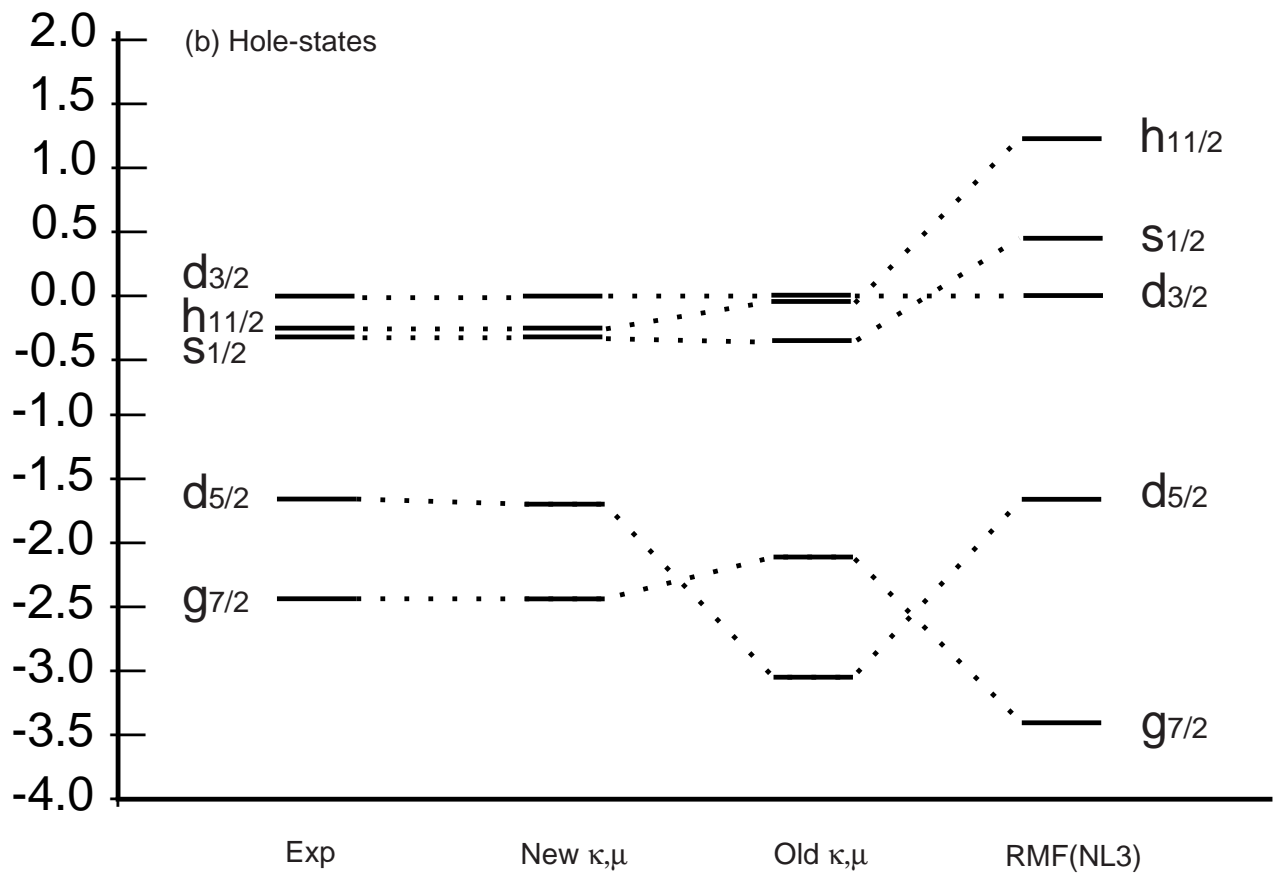


Fig. 1b, Zhang, Sun, Guidry, Riedinger, Lalazissis

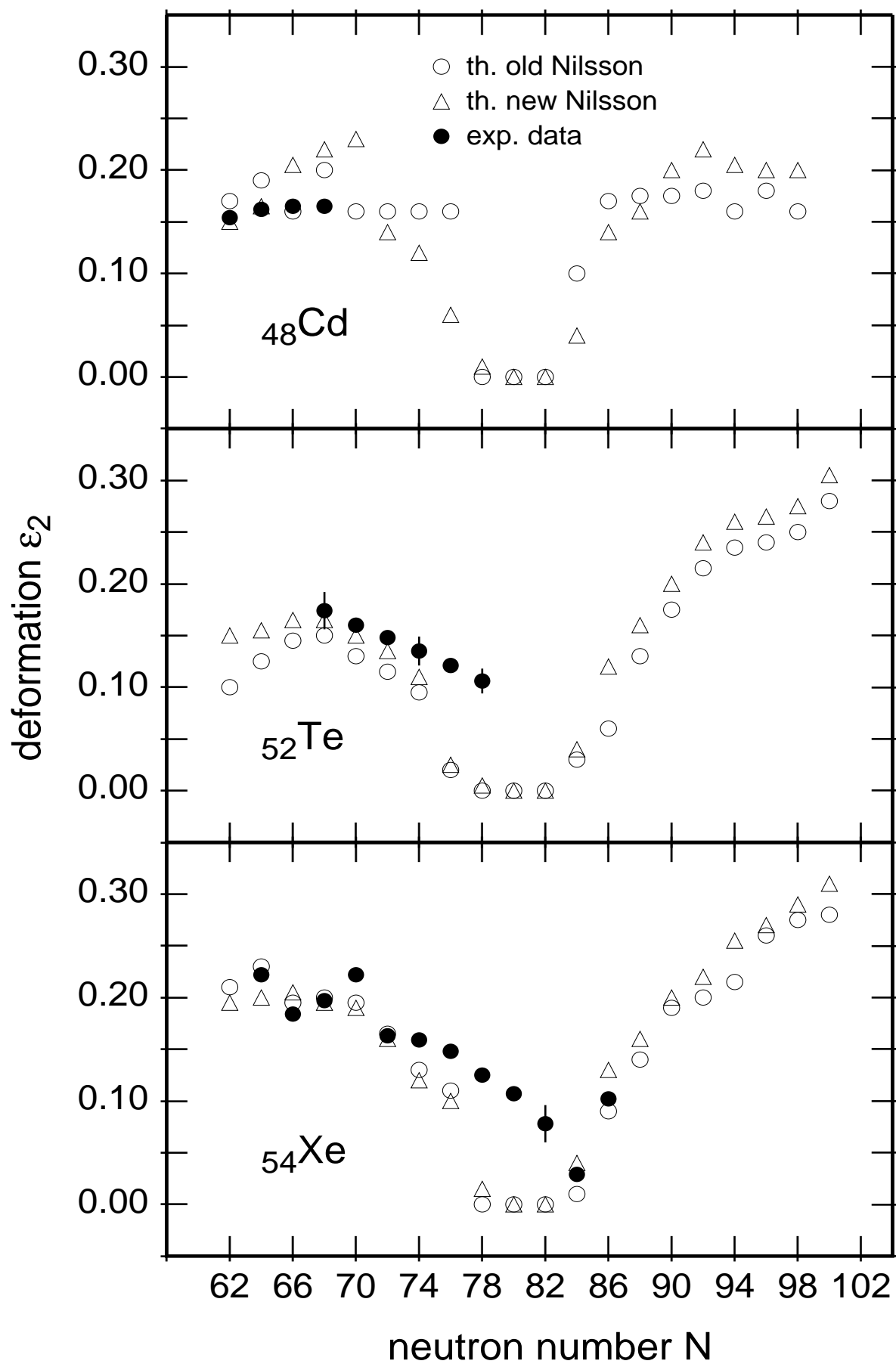


Fig. 2, Zhang, Sun, Guidry, Riedinger, Lalazissis

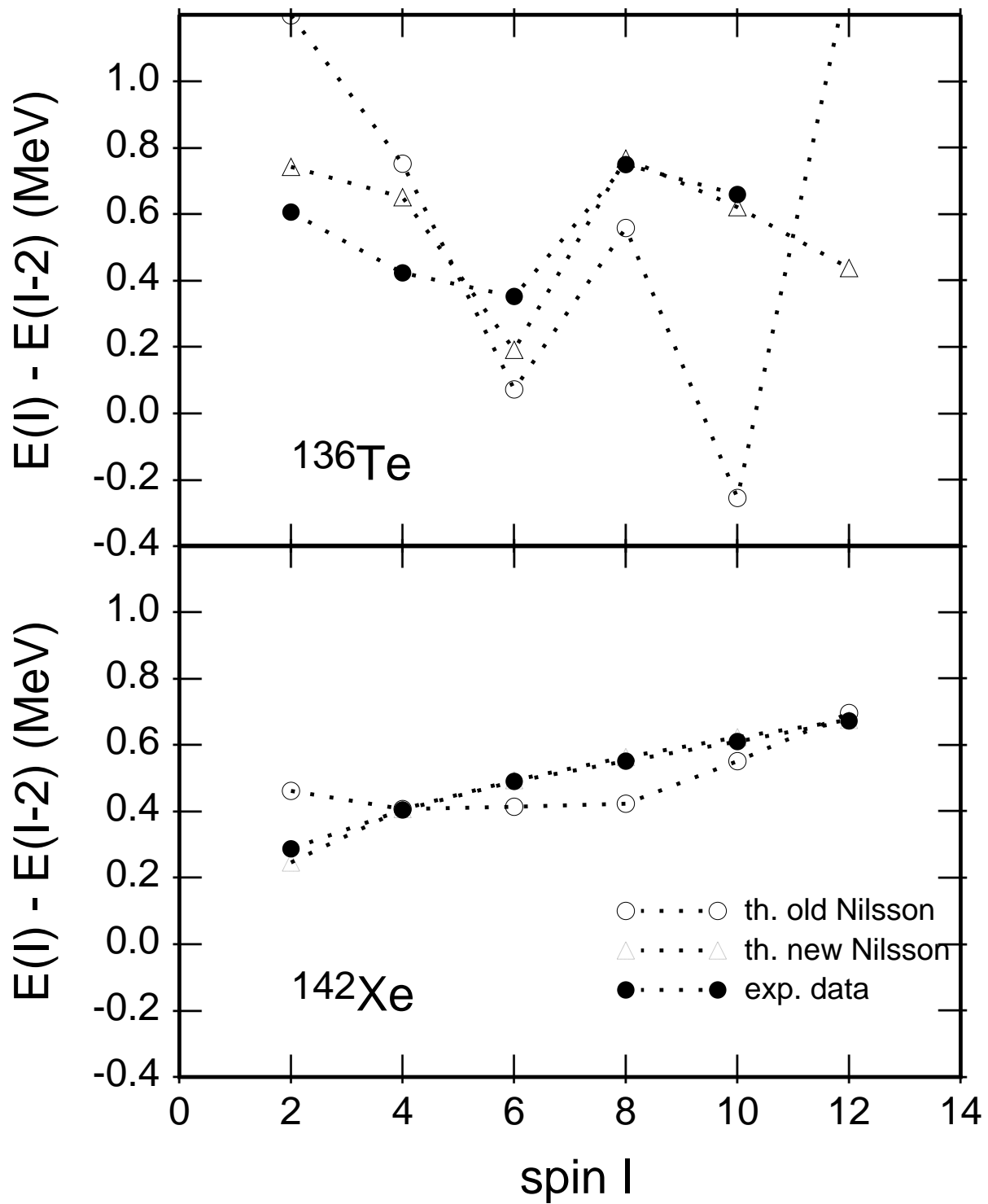


Fig. 3, Zhang, Sun, Guidry, Riedinger, Lalazissis